Molecular Basis for Nonadditive Mutational Effects in *Escherichia coli* Dihydrofolate Reductase[†]

Carston R. Wagner,[‡] Zheng Huang, Scott F. Singleton, and Stephen J. Benkovic*

Department of Chemistry, 152 Davey Laboratory, The Pennsylvania State University, University Park, Pennsylvania 16802

Received May 10, 1995; Revised Manuscript Received September 8, 1995[⊗]

ABSTRACT: Recently, two sets of single, double, and quadruple residue changes within the hydrophobic substrate binding pocket of *Escherichia coli* dihydrofolate reductase (5,6,7,8-tetrahydrofolate:NADP$^+$ oxidoreductase, EC 1.5.1.3) were shown to exhibit nonadditive mutational effects [Huang, Z., Wagner, C. R., & Benkovic, S. J. (1994) *Biochemistry 33*, 11576−11585]. In particular, the analysis of data for the L28Y, L54F, and L28Y-L54F mutations revealed nonadditive changes in the free energy associated with the substrate and cofactor binding, hydride transfer, and product release steps. Construction of a related set of mutant proteins including L28F and L28F-L54F permits a comparison of similar energy changes and provides a means for assessing differences in the interactions of Phe28 and Tyr28 with both the ligands and the side chains at residue 54. We find a single functional group change, from Phe C4-H to Tyr C4-OH, can influence the additivity of mutational effects and serve as a probe to monitor the appearance of differing enzyme conformations along the reaction pathway through changes in the interaction energy (ΔG_I). The comparison of additivity/nonadditivity in free energy changes for three interrelated double mutational cycles (WT → L28F-L54F, WT → L28Y-L54F, and L28F → L28Y-L54F) demonstrates that the side chains of positions 28 and 54 interact cooperatively to facilitate hydride transfer by preferentially influencing the enzyme−substrate ground-state complexes. The ΔG_I data for individual steps also provide evidence for multiple conformations of the enzyme operating during the catalytic cycle. The fact that there are no published examples of the synergistic enhancement of favorable mutational effects is consistent with the expectation that the binding/active site surface of wild-type dihydrofolate reductase has been optimized.

Dihydrofolate reductase (5,6,7,8-tetrahydrofolate:NADP$^+$ oxidoreductase, EC 1.5.1.3; DHFR[1]) catalyzes the NADPH-dependent reduction of 7,8-dihydrofolate (H$_2$F). The enzyme is necessary for maintaining intracellular pools of tetrahydrofolate (H$_4$F) and its derivatives, which are essential cofactors for biosynthetic reactions requiring one-carbon unit transfer. Consequently, DHFR has proven to be an attractive target for rational drug design. Structures of several binary and ternary ligand complexes of DHFR have been determined by X-ray crystallography (Bolin et al., 1982; Bystroff & Kraut, 1991; Bystroff et al., 1990; Filman et al., 1982). The elucidation of a complete kinetic mechanism (Fierke et al., 1987a; Penner & Frieden, 1987), when coupled with the structural data, has facilitated the assessment of the effects of changes within the structure of DHFR on catalysis.

The function of the residues Leu28 and Leu54, whose hydrophobic side chains comprise part of the substrate binding site of *Escherichia coli* DHFR (Figure 1), has been closely examined. The construction of a series of enzymes containing side-chain alterations at these positions by site-
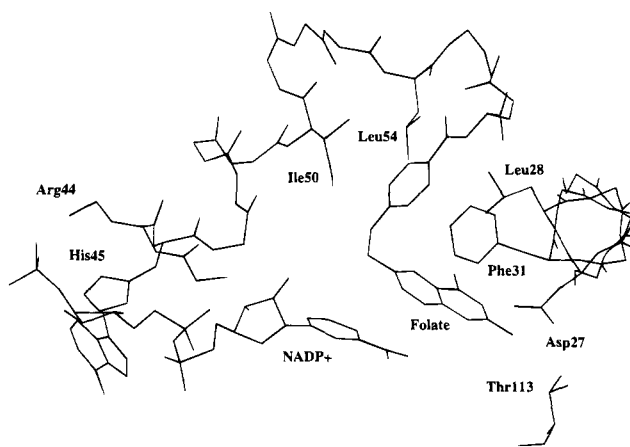

FIGURE 1: Active site of the ternary complex of *E. coli* dihydrofolate reductase with folate and NADP$^+$ (Bystroff et al., 1990).

directed mutagenesis, followed by their transient- and steady-state kinetic evaluation, has led to several important conclusions regarding the catalytic roles of these amino acids. Side-chain substitutions at the conserved residue Leu54 of *E. coli* DHFR consistently increased the barrier for hydride transfer by 2.0 kcal/mol, while the dissociation constants for H$_2$F varied by over 3 orders of magnitude, thus identifying the dominant effect of this position on the hydride-transfer step, substrate binding, and product release (Mayer et al., 1986; Murphy & Benkovic, 1989). In addition, side-chain interchange between the nonconserved residue at position 28 of *E. coli* DHFR and the analogous position of murine DHFR showed that the active site side chains impart their

characteristics individually (Wagner et al., 1992). Toward an improved understanding of this phenomenon, L28Y-L54F DHFR, containing a pair of mutations, was prepared and investigated. In contrast to the straightforward expectation based on the Leu28 substitutions, L28Y-L54F DHFR exhibited nonadditive changes in free energy for the parameters associated with ligand binding, hydride transfer, and product release in the mutational cycle WT → L28Y-L54F (Huang et al., 1994). The nonadditive effects caused by the Leu to Tyr and Leu to Phe mutations at residues 28 and 54, respectively, indicate that perturbations caused by one substitution within the hydrophobic substrate binding pocket are affected by a second mutation at another site in the pocket. Because the side chains of residues 28 and 54 reside on different substructures within the active site and are separated by ~8 Å, and since nonadditivity was observed for substrate binding and processing, it was concluded that bound substrate may communicate the coupling between the side chains.

In order to elucidate the molecular origins of the nonadditive effects within the series containing the L28Y, L54F, and L28Y-L54F mutant enzymes, we wished to analyze the kinetic and thermodynamic data obtained for the related L28F, L54F, and L28F-L54F proteins (Figure 2). Inspection of the X-ray crystallographic structures of the *E. coli* DHFR active site (Figure 1) reveals that replacement of the leucine side chain at either position 28 or 54 by a larger phenyl ring might introduce additional steric bulk into the folate-binding portion of the active site. If the basis for nonadditive changes in side-chain—side-chain interactions resides in an increase in the surface areas of the mutant enzymes' side chains compared with those of the wild-type side chains, then the combination of L28F and L54F mutations should display nonadditive effects similar to those of the L28Y and L54F mutations. Alternatively, observation of additive effects on binding and catalysis with the combination of the L28F and L54F mutations would suggest that nonadditivity in the L28Y-L54F double mutant enzyme stems from the introduction of new interactions between side chains traced to the hydroxyl moiety which is present when residue 28 is tyrosine but absent with phenylalanine. Hence, the L28F-L54F mutant enzyme was constructed by site-directed mutagenesis and characterized by steady-state and transient-state kinetic experiments. In addition, prior kinetic investigations of the L28F, L54F, and L28Y-L54F mutant enzymes performed in our laboratory were extended so that kinetic and thermodynamic parameters, and their additivity, for six DHFRs, WT, L28F, L28Y, L54F, L28F-L54F, and L28Y-L54F, could be comparatively evaluated.

The comparison of double mutational effects with those of the constituent single mutations can lend insight into the cooperative action of pairs of side chains (Horovitz & Fersht, 1990; Wells, 1990; Mildvan et al., 1992; LiCata & Ackers, 1995). In the present work, the comparison of two sets of double mutational effects (Figure 2) has provided the means to investigate the role of a simple functional group change, from Tyr C4-OH to Phe C4-H, in modulating the change in side-chain interactions. By the simultaneous evaluation of a series of double mutational cycles, the analytical method of Mildvan et al. (1992) has been extended to allow the identification of interactions between a specific pair of side chains that facilitate a particular catalytic event. An important aspect of this investigation was the ability to measure the degree of nonadditivity of mutational effects at each step

in the catalytic cycle and, thus, to draw conclusions as to the importance of changes in side-chain—side-chain and side-chain—substrate interactions in the ground and transition states. Moreover, the insertion of side-chain residues with sufficient steric bulk to affect the interaction parameter ΔG_I introduces a probe of changes in the conformational state of the protein as it cycles through its kinetic sequence. Finally, collective data from several series of multiple mutations in the substrate binding site of *E. coli* DHFR provide information on whether the side chains in the wild-type enzyme have optimized interactions for promoting binding and/or catalysis.

MATERIALS AND METHODS

Substrates and Buffers. H₂F was prepared by the dithionite reduction of folic acid (Blakley, 1960), and H₄F was prepared from H₂F by enzymatic conversion with DHFR (Mathews & Huennekens, 1960) and purified using DE-52 resin with a linear triethylammonium bicarbonate gradient (Curthoys et al., 1972). NADPH, NADP⁺, MTX, and folic acid were purchased from Sigma.

2,4-Diamino-6,7-dimethylpteridine (DAM) was purchased from ICN Pharmaceuticals. [4'(R)-²H]NADPH (NADPD) was prepared (Stone & Morrison, 1982) by using *Leuconostic mesenteroides* alcohol dehydrogenase purchased from Research Plus Inc. and purified by ion-exchange chromatography (Viola et al., 1979). Excess NaCl was removed from the purified NADPD by a Bio-Gel P-2 desalting column (Howell et al., 1987). Ligand concentrations were determined spectrophotometrically by using the following extinction coefficients: H₄F, 28 000 M⁻¹·cm⁻¹ at 297 nm, pH 7.5 (Kallen & Jencks, 1966); H₂F, 28 000 M⁻¹·cm⁻¹ at 282 nm, pH 7.4 (Dawson et al., 1969); folic acid, 27 600 M⁻¹·cm⁻¹ at 282 nm, pH 7.0 (Rabinowitz, 1960); MTX, 22 100 M⁻¹·cm⁻¹ at 302 nm in 0.1 N KOH (Seeger et al., 1949); NADPH, 6200 M⁻¹·cm⁻¹ at 339 nm, pH 7.0; NADP⁺, 18 000 M⁻¹·cm⁻¹ at 259 nm, pH 7.0. The concentrations of H₂F and NADPH were also determined by DHFR turnover.

All kinetic measurements were obtained at 25 °C in buffer containing 50 mM 2-morpholinoethanesulfonic acid (MES), 25 mM tris(hydroxymethyl)aminomethane (Tris), 25 mM ethanolamine, and 100 mM sodium chloride (MTEN buffer, pH 5—10) (Ellis & Morrison, 1982). Extensively degassed and argon-purged buffers were used in the presence of H₄F.

E. coli Strains and Biochemicals. The following strains were obtained as a gift from P. Stanssens and maintained by antibiotic selection: BMH-71 (*mutS215:Tn10*), W71-18 (*su⁻:hpsl*), and MK30—3 (*rec A⁻, su⁻*). Unless otherwise noted, all transformations were carried out according to the method of Hanahan (1983). M13K07 helper phage was obtained from Pharmacia, Inc.

Ultrapure agarose was purchased from FMC, Inc. T4 DNA ligase and T4 polynucleotide kinase were purchased from Boehringer Mannheim. Restriction endonucleases (*Cla*I and *Sma*I) were purchased from New England Biolabs Inc. Calf intestinal phosphatase was purchased from Sigma. *E. coli* DNA polymerase Pol I (Klenow fragment) was purified in our laboratory by Dr. B. Eger.

Construction of E. coli DHFR Mutant L28F-L54F. Mutagenesis was carried out as described (Wagner et al., 1992). The mutagenic oligonucleotide 5'-CGGTCGTCCGTTC-CCGGGACGC-3' (L54F) was designed to replace the codon

Table 1: Steady-State Parameters in MTEN Buffer, pH 6.0, at 25 °C

	WT	L28F[a]	L28Y	L54F	L28F-L54F	L28Y-L54F
k_{cat} (s^{-1})	12.3[b]	50	15[c]	6.3[c]	20 ± 3	13.2[c]
K_M (μM)[d]	0.7[b]	1.0	1.0[c]	0.7[c]	12 ± 4	61[c]
k_{cat}/K_M (μM^{-1} s^{-1})	18[b]	55	15[c]	9[c]	1.7 ± 0.6	0.22
$pK_a(V)$	8.4[e]	8.7	8.0 ± 0.1	8.5 ± 0.1	7.0 ± 0.1	7.8 ± 0.2
pK_a (V/K)	8.1[e]	8.5	7.0 ± 0.2	6.2 ± 0.3	6.7 ± 0.2	7.2 ± 0.2
pK_a[f]	6.5[b]	6.6	6.8 ± 0.1	7.9 ± 0.2	6.2 ± 0.1	7.0 ± 0.3
^DV	1.0[b]	1.0	1.6[c]	1.2[c]	2.0 ± 0.2	1.4[c]
^DV (pH 9.0)	2.7[b]	3.0	3.0[c]	2.7[c]	3.3 ± 0.2	3.0[c]

[a] Data taken from Wagner et al. (1992). [b] Data taken from Fierke et al. (1987a). [c] Data taken from Huang et al. (1994). [d] The K_M is that for dihydrofolate. [e] Data taken from Stone and Morrison (1982). [f] Except for the wild-type value taken from Fierke et al. (1987a), the pK_a values were determined from DAM inhibition studies as described in the text.

for leucine (TTG) with that for phenylalanine (TTC) and incorporate a unique *Sma*I restriction site. The template single-stranded DNA was generated from the plasmid containing the *E. coli* L28F mutant protein rather than from the plasmid containing the wild-type gene. The efficiency of mutagenesis was approximately 95%.

Protein Purification. Strain MK30-3 was transformed with the plasmid for the *E. coli* L54F or L28F-L54F mutant protein. Single colonies were selected and grown in small culture [10 mL, LB, chloramphenicol (50 μg/mL); trimethoprim (20 μg/mL)] to an $OD_{600} \approx 1.5$, followed by dilution into 1 L of LB (chloramphenicol, 50 μg/mL) and grown to $OD_{600} \approx 1.5$. The cells were collected by centrifugation, and protein purification was carried out as described by Baccanari et al. (1977) and Chen et al. (1985) with one exception. The L54F protein was eluted by increasing the pH of the column buffer from 6.0 to 9.0 without the addition of folate. The procedure routinely yielded 8–10 mg of purified protein/g of cells.

Steady-State Kinetics. Initial velocities for the enzyme reactions were measured by using either a Gilford or Cary 219 UV–visible spectrophotometer at 25 °C. The molar absorbance change used was 11 800 M^{-1}·cm^{-1} (Stone & Morrison, 1982). DHFR was preincubated with varying amounts of NADPH before H$_2$F was added to remove hysteretic effects (Penner & Frieden, 1985). The intrinsic pK_a's of the enzymes were determined from DAM inhibition studies as previously described by Stone and Morrison (1982).

Fluorescence Titrations. The thermodynamic dissociation constants (K_D) for ligands binding to the mutant DHFRs were measured by fluorescence titration at 25 °C on a SLM 8000 spectrofluorometer. Quenching of the intrinsic enzyme fluorescence at 340 nm upon excitation at 290 nm was monitored as a function of ligand concentration (Birdsall et al., 1980; Stone & Morrison, 1982; Taira & Benkovic, 1988). Standard tryptophan solutions were used to correct for ligand internal filter effects. The enzyme concentration used was either at or slightly less than the K_D value of the ligand. The data were fit by a nonlinear least squares fitting program previously described (Taira & Benkovic, 1988).

Transient and Pre-Steady-State Kinetics. Transient binding and pre-steady-state kinetic experiments were performed on an Applied Photophysics Inc. stopped-flow spectrophotometer. The instrument is capable of absorbance and fluorescence measurements at 25 °C and fit with a monochrometer for generating the excitation input. They both have a 2 mm or 10 mm cell path length from which either fluorescence or transmittance can be observed with a dead time less than 2 ms. In most cases, ligand binding experi-

ments were monitored by excitation of DHFR fluorescence at 290 nm and observation of the degree of quenching at 340 nm by using an output bandpass filter with a range of 250-400 nm. Coenzyme fluorescence was measured at 450 nm using a 400 nm cutoff filter. Absorbance measurements were monitored at 340 nm using the 250–400 nm bandpass filter. Typically, three to six traces were recorded and averaged for future data analysis.

After the trigger impulse, data were collected over a preselected time range from 5 ms to 15 min. Kinetic data were fit using a nonlinear least squares computer program provided by Applied Photophysics, Inc. A transient was analyzed as either a single exponential or a single exponential followed by a linear rate.

Kinetic Simulations. Kinetic simulations were performed by the computer simulation program KINSIM (Barshop et al., 1983), modified by K. Johnson and J. Wagner on a VAX microcomputer or with HopKINSIM on a Macintosh microcomputer as modified by D. Wachsstock.

RESULTS

Steady-State Kinetic Parameters. The steady-state parameters k_{cat} and K_M were determined as a function of pH by varying the H$_2$F concentration (1–80 μM) while holding constant the NADPH concentration (100 μM) (Table 1). Doubling the NADPH concentration had no effect on the observed rates of these reactions for the L28F-L54F mutant protein.

As demonstrated previously for wild-type *E. coli* (Fierke et al., 1987a) and other mutant DHFRs (Adams et al., 1991; Benkovic et al., 1988; Fierke & Benkovic, 1989; Murphy & Benkovic, 1989; Taira & Benkovic, 1988; Wagner & Benkovic, 1992), the reaction catalyzed by the L28F-L54F mutant enzyme exhibited a strong pH dependence. A maximum rate was reached as the pH decreased, implying that turnover is facilitated by the preprotonation of a residue at the active site. Analysis of the V and V/K profiles in terms of a single pK_a gave satisfactory fits to the observed data, yielding the values shown in Table 1. Also included in Table 1 are the deuterium isotope effects on V at low and high pH with saturating [4'(R)-^{2}H]NADPH, showing the chemical step to be predominantly rate limiting at high pH.

Thermodynamic Dissociation Constants (K_D). The binding of H$_2$F and NADPH to free DHFR was examined by following the decrease in enzyme fluorescence that occurs upon formation of DHFR–ligand complexes (Taira & Benkovic, 1988). The K_D values for H$_2$F and NADPH are given in Table 2 for the mutant enzymes. Although substrate

Table 2: Thermodynamic Dissociation Constants[a]

	WT[b]	L28F[c]	L28Y[d]	L54F[d]	L28F-L54F	L28Y-L54F[d]
K_D (μM) (NADPH)	0.33	0.40	0.15	0.17	3.5 ± 0.7	0.60
K_D (μM) (H$_2$F)	0.22	0.15	0.11	0.10	0.2 ± 0.05	11

[a] Measured using fluorescence quenching titrations. [b] Data taken from Fierke et al. (1987a). [c] Data taken from Wagner et al. (1992). [d] Data taken from Huang et al. (1994).

binding was unaltered, the K_D for cofactor binding to the L28F-L54F mutant enzyme increased approximately 10-fold.

Binding Kinetics by the Relaxation Method. Stopped-flow quenching of the intrinsic enzyme fluorescence has been used to measure the association and dissociation rate constants of ligands to wild-type and several mutant DHFRs (Adams et al., 1989; Appleman et al., 1990; Cayley et al., 1981; Dunn & King, 1980; Fierke et al., 1987a). The association and dissociation rate constants for cofactor binding to the free L28F-L54F mutant enzyme were $16.8 \pm 1.6 \mu M^{-1} s^{-1}$ and $32.5 \pm 17.9 s^{-1}$, respectively. The value for the off rate corresponds closely to the value $41 \pm 7 s^{-1}$ determined by the competition method (Table 2). Conversion of E_2 to E_1 proceeded with a rate constant of $0.064 \pm 0.004 s^{-1}$ for the L28F-L54F mutant enzyme. The value is similar to the rate constant of $0.034 s^{-1}$ observed for the wild-type enzyme. Nevertheless, the K_{eq} value for the L28F-L54F mutant protein increased by 2.9-fold.

The K_D for NADPH is related to k_{on} and k_{off} by eq 1 (Fierke et al., 1987a). In support of the above binding mechanism,

$$K_D = k_{off}/k_{on}[1 + 1/K_{eq}]   \qquad (1)$$

the calculated K_D for the L28F-L54F mutant enzyme was 3.61 μM, which is also in fair agreement with the observed value of 3.45 μM.

Accurate values for the association and dissociation rate constants for H$_2$F were not obtained owing to the lack of significant fluorescence quenching for both proteins.

Dissociation Rate Constants by the Competition Method. The dissociation rate constants for ligands from wild-type and mutant DHFRs can also be measured by a method of competition (Dunn & King, 1980; Fierke et al., 1987b). The values for several ligands to both binary and ternary complexes of the mutant DHFRs are shown in Table 3.

Pre-Steady-State Kinetics. For the wild-type enzyme and all of the mutant proteins except L28F-L54F, the observed rates of hydride transfer from NADPH to H$_2$F given in Table 4 were measured from pre-steady-state transients as described earlier (Huang et al., 1994). To determine the rate constant for hydride transfer from the protonated ternary complex (H·E·NH·H$_2$F) and thus the intrinsic pK_a of the complex, the pH-dependence of the observed hydride transfer rate constant was measured. The data were then fit to eq 2,

$$k_{obs} = k_H/(1 + K_a/[H^+])   \qquad (2)$$

yielding the intrinsic pK_a and pH independent hydride transfer rate. The pK_a values measured in this way were consistent with those determined by DAM titration (Stone & Morrison, 1983).

Unfortunately, the rate of hydride transfer for the L28F-L54F mutant enzyme could not be accurately determined

by the above methodology. Nevertheless, by use of eq 2 with the k_{obs} values and intrinsic pK_a measured by DAM titration, a value of $126 \pm 25 s^{-1}$ was estimated for the pH-independent rate of hydride transfer for the L28F-L54F double mutant protein.

Reverse Hydride-Transfer Rate Constants. The reverse rates of the reaction (i.e., net conversion of H$_4$F and NADP$^+$ to H$_2$F and NADPH) for the L54F and L28F-L54F mutant enzymes were measured by monitoring the increase in absorbance at 340 nm in a reaction solution containing degassed MTEN buffer, 200 μM H$_4$F, 2 mM NADP$^+$, 0.1 M NaCl, and 3 mM DTT at pH 10.0, 25 °C (Table 4). Doubling of the substrate concentration or decreasing the buffer pH to 9.0 had virtually no effect on the observed rates of these reactions.

Kinetic Simulations. As a check on the individually determined rate constants, the steady-state parameters, k_{cat} and K_M, for the L28F-L54F mutant enzyme, were calculated for the minimal kinetic model shown in Scheme 1 by computer simulation. Where appropriate, the independently determined rate constants were employed. Because the mutant enzymes had little effect on the association rate constant of NADPH for the free enzyme, the rate constants for the association of NADP$^+$ and NADPH for the E·H$_4$F complex (i.e., k_{-3} and k_4) were assumed to be equivalent to the values obtained for wild-type. In the absence of directly determined association rate constants for H$_2$F binding to the L28F-L54F mutant protein, a value of 5 $\mu M^{-1} s^{-1}$, was estimated from the K_D and k_{off} values measured from the E·H$_2$F complex. The calculated steady-state parameters were in satisfactory agreement with the measured values within experimental error.

DISCUSSION

The insights gained from investigations of single mutant proteins may be elaborated further by studies of double mutant proteins which can provide information on the cooperative action of pairs of side chains (Horovitz & Fersht, 1990; Wells, 1990; Mildvan et al., 1992; LiCata & Ackers, 1995). The double mutant enzyme L28Y-L54F exhibits nonadditive mutational effects on binding and catalysis (Huang et al., 1994). In order to elucidate the molecular origins of these nonadditive effects, we have compared the kinetic and thermodynamic parameters for the following mutant DHFRs: L28Y, L28F, L54F, L28F-L54F, and L28Y-L54F. Our analytical approach, which is based on a series of proteins containing common mutations (Figure 2), however, is not restricted to these specific changes but should be generally applicable to the evaluation of the effects of multiple mutations on the binding and kinetic parameters for any enzyme.

Energetic Perturbations of the Catalytic Cycle by Mutations at Positions 28 and 54. The mechanistic framework for *E. coli* DHFR contains the following key features (Fierke et al., 1987a): (1) H$_4$F release limits steady-state turnover at neutral pH; (2) the preferred pathway for H$_4$F release is from the mixed ternary E·NH·H$_4$F complex; and (3) the overall reaction strongly favors H$_4$F formation due in part to the high value associated with the internal equilibrium for the reactive ternary complex. Due to their importance in the catalytic function of DHFR, six thermodynamic and kinetic parameters were evaluated for each enzyme: the

Table 3: Dissociation Rate Constants [k_{off} (s^{-1}) at pH 6.0, 25 °C][a]

| ligand	enzyme species	WT[b]	L28F[c]	L28Y	L54F	L28F-L54F	L28Y-L54F[d]
NADPH	E	3.6	2.5	5.4[d]	3.3[d]	41 ± 7	6.4
	E·H$_4$F	85	8.0			90 ± 14	
NADP$^+$	E	290	157			264 ± 11	
	E·H$_4$F	200	287	103[d]	232[d]	233 ± 4	40
H$_2$F	E	22	90	22 ± 2	2 ± 1	0.89 ± 0.16	
H$_4$F	E	1.4	40	37[d]	2.1[d]	32 ± 5	21
	E·NADPH	12	80	21[d]	13[d]	48 ± 4	21
	E·NADP$^+$	2.4	34				

[a] Kinetic constants derived from competition experiments. [b] Data taken from Fierke et al. (1987a). [c] Data taken from Wagner et al. (1992). [d] Data taken from Huang et al. (1994).

Table 4: Forward and Reverse Hydride Transfer Rate Constants

	WT[a]	L28F[b]	L28Y	L54F	L28F-L54F	L28Y-L54F
k_{hyd} (s^{-1})	950	4000	109[c]	20.0[c]	126 ± 25	77[c]
k_{rev} (s^{-1})	0.60	0.56	0.25 ± 0.02	0.013 ± 0.001	0.036 ± 0.002	0.0049 ± 0.001
K_{int}	1600	7000	440	1500	3500	16000

[a] Data taken from Fierke et al. (1987a). [b] Data taken from Wagner et al. (1992). [c] Data taken from Huang et al. (1994).

Scheme 1
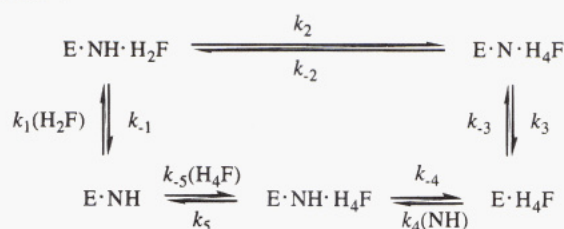
thermodynamic dissociation constants for H$_2$F and NADPH from the corresponding binary complexes, the forward and reverse hydride transfer-rates, the internal equilibrium constant, and the rate constant for product release.

For each of these six key properties, the energetic perturbation effected by each single and double mutation at positions 28 and 54 relative to the wild-type enzyme was calculated using the equations

$$\Delta\Delta G_D = -RT \ln(K_{D,wt}/K_{D,mt}) \quad (3a)$$

$$\Delta\Delta G_{int} = -RT \ln(K_{int,mt}/K_{int,wt}) \quad (3b)$$

$$\Delta\Delta G^{\ddagger} = -RT \ln(k_{mt}/k_{wt}) \quad (3c)$$

where $\Delta\Delta G_D$, $\Delta\Delta G_{int}$, and $\Delta\Delta G^{\ddagger}$ represent the differences in free energy changes associated with a binding constant, the internal equilibrium constant, and a rate constant, respectively, for a mutant enzyme (mt) relative to the wild-type enzyme (wt). On the basis of the sign convention of eq 3, a negative $\Delta\Delta G$ indicates that the mutant enzyme has improved binding, a more favorable equilibrium, or an increased rate constant. The calculated mutational effects are summarized graphically in Figure 3. Although the mutations generally improve substrate binding and product dissociation while decreasing both forward and reverse hydride transfer rates, the free energy perturbations imparted by the L28F and L28Y substitutions in the single and double mutant enzymes are not identical. Interestingly, all of the mutant proteins except L54F display an increased H$_4$F dissociation rate, whereas only the L28F mutant enzyme has an increased hydride transfer rate.
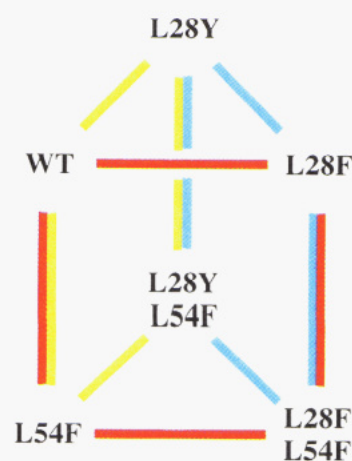

FIGURE 2: Interrelatedness between wild-type and mutant enzymes in each of three sets. Enzymes related by single amino acid changes are connected by single line segments, with the color of the line segment (red, green, or blue) corresponding to one of three mutagenic cycles. The wild-type enzyme has Leu residues at both positions 28 and 54.

Evaluation of Changes in Side-Chain Interaction Energies. The thermodynamic perturbation of a protein's functional property by a pair of mutations can be expressed by the free energy relationship:

$$\Delta\Delta G_{(X,Y)} = \Delta\Delta G_{(X)} + \Delta\Delta G_{(Y)} + \Delta G_I \quad (4)$$

where $\Delta\Delta G_{(X)}$ and $\Delta\Delta G_{(Y)}$ are the free energy changes caused by single mutations at positions X and Y, respectively, $\Delta\Delta G_{(X,Y)}$ represents the free energy change observed for the double mutant protein, and ΔG_I is the change in the interaction energy between the side chains at X and Y (Wells, 1990; LiCata & Ackers, 1995). When the change in interaction energy, or degree of coupling, between two side chains in an active site is negligible ($\Delta G_I \approx 0$), the effect of each mutation is independent of the other and their energetic impacts are additive. If, however, $\Delta G_I \neq 0$, then the mutational effects are nonadditive and the influence of each mutation at one position depends on the side chain present at the second position. In fact, Mildvan and co-workers have shown that quantitative comparisons of the sign and magnitude of $\Delta\Delta G_{1+2}$ with those of $\Delta\Delta G_1 + \Delta\Delta G_2$ and $\Delta\Delta G_1$,
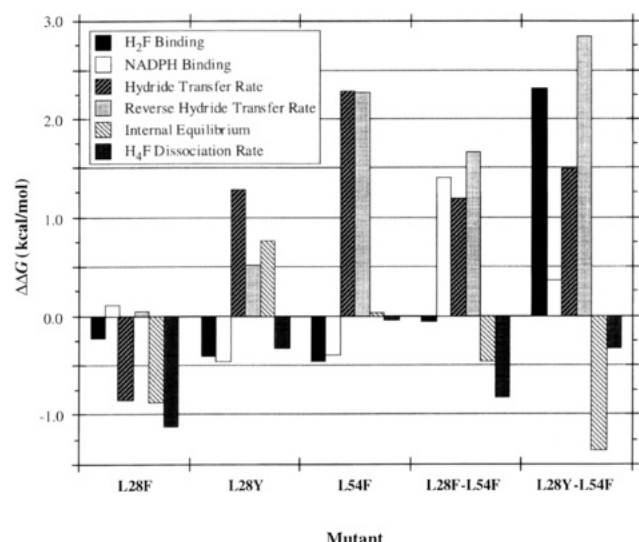
FIGURE 3: Differences in free energy changes ($\Delta\Delta G$ or $\Delta\Delta G^{\ddagger}$) for the binding ($K_D$) of H_2F or NADPH, for the rate constants for forward (k_{hyd}) or reverse (k_{rev}) hydride transfer, for the internal equilibrium associated with the hydride transfer step (K_{int}), or for the rate constant for H_4F dissociation (k_{off}) relative to the wild-type enzyme. Calculations were done using eq 3. Propagation of the uncertainty in each equilibrium or rate constant to the corresponding $\Delta\Delta G$ yields an estimated uncertainty of ≤ 0.6 kcal/mol in the plotted values.
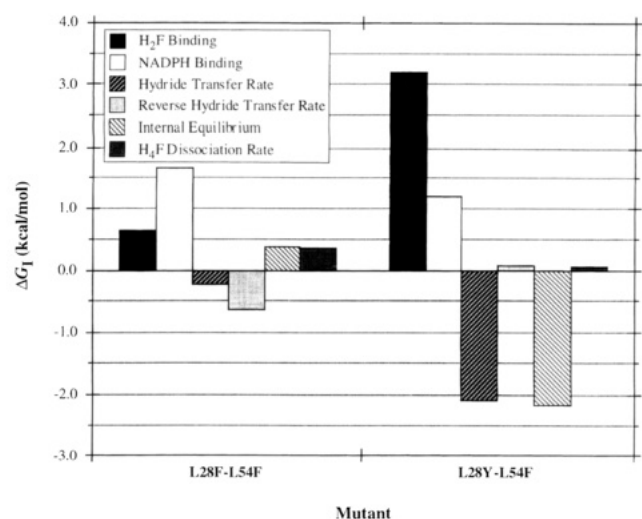

FIGURE 4: Side-chain coupling free energies (ΔG_I) for the double mutants L28F-L54F and L28Y-L54F. Calculations were done using eq 4 and the known differences in free energy changes for each mutant enzyme (Figure 3). On the basis of the error analysis described for Figure 3, the estimated error for each ΔG_I value is ≤ 1.0 kcal/mol.

where $\Delta\Delta G_1$, $\Delta\Delta G_2$, and $\Delta\Delta G_{1+2}$ are the free energy perturbations caused by the single mutation having the larger effect, the single mutation having the smaller effect (*i.e.*, $|\Delta\Delta G_1| > |\Delta\Delta G_2|$), and the double mutant protein, respectively, reveal the cooperative or anticooperative nature of side-chain interactions in a particular process (Mildvan et al., 1992).

In order to assess changes in the degree of coupling between the side chains at positions 28 and 54, ΔG_I was calculated for both double mutant enzymes (Figure 4). As was previously demonstrated, the L28Y-L54F mutant enzyme displays a substantial change in the coupling between the side chains at positions 28 and 54 relative to wild type, particularly for the ligand binding and hydride-transfer steps

(Huang et al., 1994). In contrast, the perturbations imparted by the phenylalanines at position 28 and 54 are additive within experimental error with regard to both the binding of substrate and product and the forward and reverse hydride-transfer rates but nonadditive with respect to cofactor binding. Although the L28F and L54F mutations have only modest effects on cofactor binding, the stability of the E·NH complex is dramatically reduced by the combination of mutations in the double mutant enzyme. Overall, the contrasting pattern exhibited in Figure 4 suggests that the change from a hydrogen (phenylalanine C4-H) to a hydroxyl group (tyrosine C4-OH) can substantially alter both the magnitude and type of interactions between active site residues. Interestingly, a preliminary analysis of X-ray crystallographic structures of the binary MTX complexes of L28F and L28Y mutant DHFRs reveals that, although the folate binding site can tolerate either phenylalanine or tyrosine at position 28, the phenyl ring of the side chain adopts different conformations in the two complexes (Professor Katherine A. Brown, personal communication).

Comparison of Changes in Interaction Energies between Double Mutant Proteins. By comparing the kinetic and thermodynamic parameters of two sets of mutant proteins which involve two different mutations at position X and a common mutation at position Y, one may obtain a quantitative measure of the degree to which this common amino acid modulates the difference in the perturbations caused by the amino acid changes at position X. Recall that the changes in side-chain coupling for the two pairs of mutations are given by $\Delta G_I = \Delta\Delta G_{(X^2,Y)} - \Delta\Delta G_{(X^2)} - \Delta\Delta G_{(Y)}$ and $\Delta G_I = \Delta\Delta G_{(X^1,Y)} - \Delta\Delta G_{(X^1)} - \Delta\Delta G_{(Y)}$, where the terms are equivalent to those defined for eq 3 and the superscripts on X indicate the different mutations at this position. The free energy associated with the influence of the mutation at position Y is then given by

$$\Delta\Delta G_I = [\Delta\Delta G_{(X^2,Y)} - \Delta\Delta G_{(X^1,Y)}] - [\Delta\Delta G_{(X^2)} - \Delta\Delta G_{(X^1)}] \quad (5)$$

The difference expressed by eq 5 is a change in the interaction energy between positions X and Y when the first mutant amino acid is changed to the second at position X and the wild-type amino acid is replaced at position Y. Importantly, because eq 5 represents a measure of nonadditivity in the $(X^1) \rightarrow (X^2Y)$ double mutation, the effects can be quantitatively interpreted as for any other double mutational effect (see discussion above). The analogy between $\Delta\Delta G_I$ and ΔG_I is apparent when amino acid 1 at position X is simply the wild-type side chain. For this case, the second term of the right-hand side of eq 5 represents a single mutation (i.e., $\Delta\Delta G_{(X^1,Y)} \rightarrow \Delta\Delta G_{(Y)}$, the fourth term is equal to zero by definition, and $\Delta\Delta G_I = \Delta G_I$. Because the analysis is general for double mutations, the data encompass three cases (Figure 2): (1) the effect of substituting phenylalanine for leucine at position 54 on the perturbation imparted by the substitution of phenylalanine for the wild-type leucine residue at position 28 (WT $\rightarrow$ L28F-L54F); (2) the effect of the Leu54 to Phe54 change on the perturbation imparted by the substitution of tyrosine for the wild-type leucine residue at position 28 (WT $\rightarrow$ L28Y-L54F); and (3) the effect of the Leu54 to Phe 54 change on the substitution of tyrosine for phenylalanine at position 28 (L28F $\rightarrow$ L28Y-L54F). The free energy perturbations associated with the essential kinetic
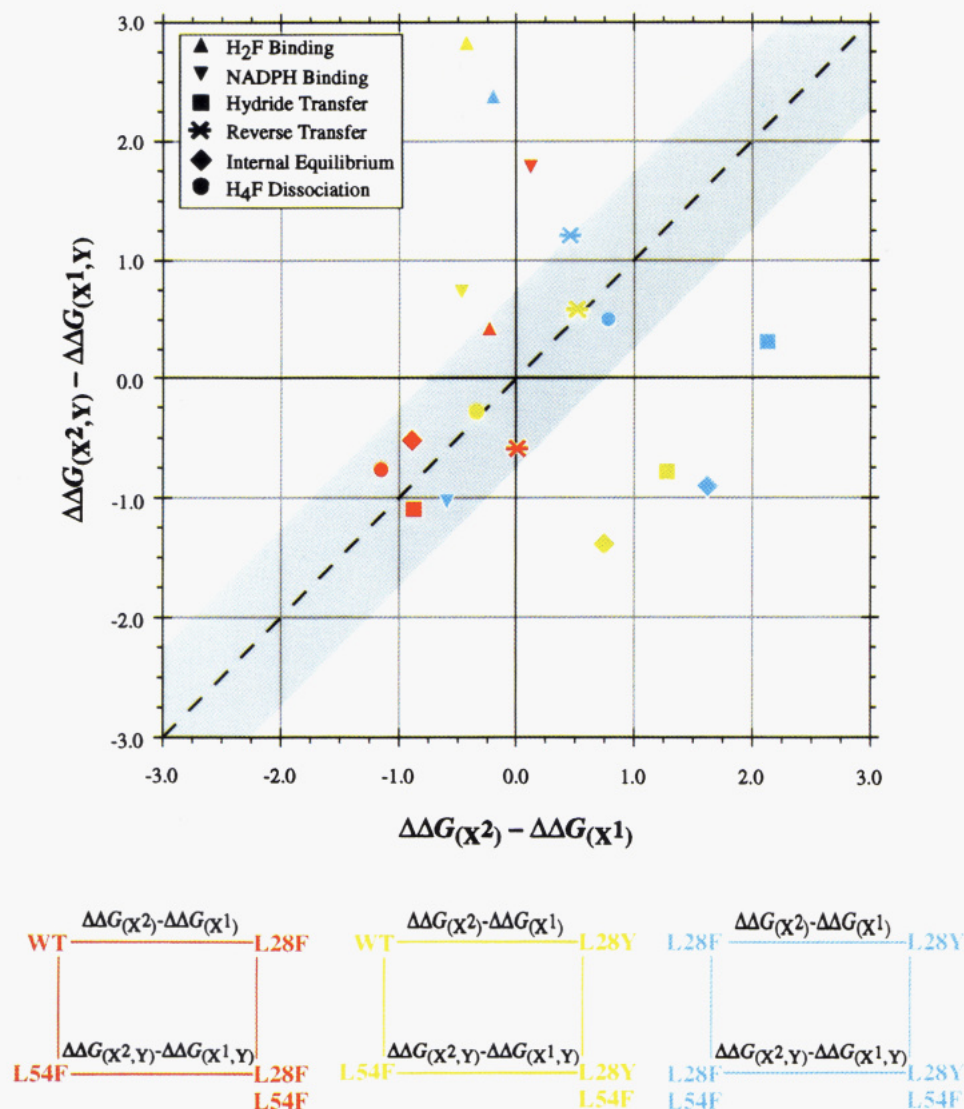
FIGURE 5: Plot of the influence of a mutation at position 54 on the energetic perturbation associated with a mutation at position 28. The vertical coordinate ($\Delta\Delta G_{(X^2,Y)} - \Delta\Delta G_{(X^1,Y)}$) represents the energetic change caused by an amino acid substitution at position 28 in the presence of a mutation at position 54, while the horizontal coordinate ($\Delta\Delta G_{(X^2)} - \Delta\Delta G_{(X^1)}$) represents the effect of the change at position 28 alone. The colors of the symbols are the same as the colors of the line segments connecting mutationally related enzymes in Figure 2: red symbols represent the WT → L28F-L54F mutational cycle, green symbols represent the WT → L28Y-L54F mutational cycle, and blue symbols represent the L28F → L28Y-L54F mutational cycle. The dashed diagonal line indicates the expected position of data points corresponding to additive mutational effects on a given equilibrium or rate constant. The diagonal gray band indicates the uncertainty in the data. On the basis of the error analysis described in Figure 3, the band corresponds to the region wherein *either* coordinate's value is within 0.8 kcal/mol of the dashed line. Hence, data points falling within the gray region represent mutational effects that are additive within experimental uncertainty.

and thermodynamic parameters for the three cases were calculated and are depicted graphically in Figure 5.

In general, the replacement of leucine at either position 28 or 54 with aromatic side chains provides slightly improved interaction with H_2F. The data point for the WT → L28F-L54F cycle lies within the diagonal band of Figure 5 ($\Delta G_I \approx 0$), indicating that Phe28 and Phe54 are not interacting differently than wild-type residues in this step. The introduction of Phe54 in the WT → L28Y-L54F or L28F → L28Y-L54F cycle reverses the slightly beneficial effect of substituting tyrosine for leucine or phenylalanine at position 28 on the K_D (H_2F). This results in a strong advantage for phenylalanine relative to tyrosine at position 28 in H_2F binding when phenylalanine is at position 54. The antagonism between Tyr28 and Phe54 suggests that the specific combination of side chains found with the L28Y-L54F double mutant protein sterically crowds the substrate binding

site and reduces the conformational flexibility needed to accommodate H_2F. The hydroxyl group of the tyrosine would appear to be a necessary element for this antagonism.

For K_D (NH) in the L28F → L28Y-L54F cycle, the point falls close to the diagonal, indicating that the side chains of residue 54 (Leu or Phe) have similar effects on the perturbation caused by a phenylalanine to tyrosine change at position 28 ($\Delta\Delta G_I \approx 0$). Although the effects on cofactor binding of changing residue 28 from leucine to phenylalanine or tyrosine are antagonistic with that of the Leu54 to Phe mutation [$\Delta\Delta G_D$ (NH) $\leq$ 0 for the single mutant proteins and $\Delta\Delta G_D$ (NH) $>$ 0.3 for the double mutant enzymes (Figure 3)], tyrosine at position 28 stabilizes the E·NH complex more than phenylalanine, independent of the side chain at position 54. Hence, the improved binding exhibited by enzymes with tyrosine rather than phenylalanine at position 28 results from improved interactions with the

cofactor rather than changes in side-chain coupling. These interactions occur despite the loci of the changes being in the folate binding site.

The three cycles exhibit differing effects on k_{hyd}. The data point for the WT → L28F-L54F cycle lies close to the diagonal ($\Delta G_I \approx 0$), and the absence of side-chain interaction changes for this step (Figure 4) leads to the conclusion that the F28/F54 interaction energy is not different from the wild type. On the other hand, the two other cycles, WT → L28Y-L54F and L28F → L28Y-L54F, have data points off the diagonal, indicating changes in side-chain interactions. The introduction of phenylalanine at position 54 in the latter cycle slightly reduces the unfavorable effect of the F28Y switch. The fact that the effects of the Phe28 to Tyr28 and Leu54 to Phe54 changes are partially additive (L28F → L28Y-L54F cycle) indicates that Phe28 and Leu54 may act cooperatively in facilitating forward hydride transfer relative to the side-chain combination of Tyr28 and Phe54 (Mildvan et al., 1992). Moreover, because the changes in interaction energies along the WT → L28Y-L54F and L28F → L28Y-L54F mutational cycles are the same within experimental error, the wild-type residues at positions 28 and 54 may also act cooperatively in this step. Taken together, these observations suggest that L28F achieves an increased hydride-transfer rate by altered interactions with the ligands rather than the side chain at position 54 (Wagner et al., 1992). Significantly, the three cycles yield data points for k_{rev} that are within experimental error of the diagonal so that $\Delta\Delta G_I \approx 0$, suggesting that the side-chain interactions in this step for all combinations are similar to those of wild type. Since $\Delta G_I \approx 0$ for k_{rev} in the two double mutant proteins (Figure 4), we conclude that the differences in the side-chain interactions observed in k_{hyd} and not in k_{rev} must arise from an effect within the E·NH·H$_2$F complex that is not expressed in the common transition state which links these two kinetic steps.

As anticipated, the internal equilibrium (K_{int}) data point for the WT → L28F-L54F cycle lies close to the diagonal while the data points for WT → L28Y-L54F and L28F → L28Y-L54F indicate a change in side-chain coupling. In the latter case, the substitution of phenylalanine for leucine at position 54 compensates for the unfavorable effect of the F28Y change. The data points for k_{hyd} and K_{int} for a given cycle lie within experimental error of one another, thus verifying our analysis that the effect of the differences in side-chain coupling is primarily expressed in the ground state of the E·NH·H$_2$F complex.

Finally, the interaction energy changes in the k_{off} (H$_4$F) for the three cycles lie close to the diagonal so $\Delta\Delta G_I \approx 0$. Changing phenylalanine to tyrosine at position 28 results in a small decrease in k_{off} (H$_4$F), independent of whether there is a leucine or phenylalanine at position 54. Conversely, L54F has little influence on k_{off} (H$_4$F) either alone or in combination with the side-chain changes at position 28. Generally, mutations that facilitate substrate binding also facilitate product release and vice versa (the exception being the combination of side-chain changes in L28Y-L54F; Figure 3).

Conformational Change during the Catalytic Cycle. While the preceding discussion indicates the generality of nonadditive mutational effects in the substrate binding site, the degree of interaction energy changes varies from parameter to parameter. This effect can be seen most clearly in the

data of Figure 4. The appearance of substantial but differing values for ΔG_I that are dependent on the identity of the kinetic step suggests that the degree of the side-chain interaction has been altered in response to changes in the enzyme's conformational state accompanying that step. In particular, mutational effects on substrate binding and forward hydride transfer are generally characterized by changes in side-chain coupling while the same amino acid changes have additive effects on reverse hydride transfer, the internal equilibrium, and product dissociation. Hence, the ground-state substrate complexes, E·H$_2$F and E·H$_2$F·-NH, are sensitive to changes in side-chain coupling caused by mutations while the product complexes, E·H$_4$F·N$^+$ and E·H$_4$F·NH, and the transition state for hydride transfer are not. The simplest explanation for these observations is that the product complexes of wild-type and mutant enzymes have conformations that sever the particular interactions between side chains at positions 28 and 54.

Multiple Mutations of E. coli DHFR: Implications for Catalysis and Evolution. In addition to Leu28 and Leu54, two other residues within the hydrophobic substrate-binding pocket of *E. coli* DHFR have been extensively characterized by site-directed mutagenesis and kinetic evaluation with respect to their roles in substrate binding and catalysis. These residues, Phe31 and Ile50 (Figure 1), have also been studied as components of two additional sets of multiple mutations within the H$_2$F-binding site: F31V/L54G/F31V-L54G (Mayer et al., 1986; Chen et al., 1987; Taira et al., 1987; Murphy et al., 1989; Wagner & Benkovic, 1990) and L28A-F31A/I50A-L54G/L28A-F31A-I50A-L54G (Huang et al., 1994). In order to examine the additivity in terms of the changes in free energy of key thermodynamic and kinetic parameters of the mutations within the three sets reported here (Figure 2) as well as the two involving Phe31 and Ile50, we have plotted ($\Delta\Delta G_{1+2} - \Delta\Delta G_1$) *versus* $\Delta\Delta G_2$ for all five mutational cycles (Figure 6).

Taken together, the data represented in Figure 6 offer a number of conclusions regarding the additivity of mutational effects within the substrate-binding site of DHFR. For both substrate and cofactor binding, the effect of a second mutation is generally to antagonize the effect of the first, resulting in an overall decrease in affinity for the ligand. However, when one of the mutations is a side-chain deletion (*i.e.*, replacement by glycine), the effect of the second mutation is to suppress the reduction in affinity so that K_D for the double mutant enzyme is closer to the wild-type parameter than would be expected from the sum of the single mutational effects [$0 < \Delta\Delta G_{1+2}/(\Delta\Delta G_1 + \Delta\Delta G_2) < 1$]. Although the influence of the mutations on K_D (H$_2$F) is generally larger than that on K_D (NH), both substrate and cofactor binding are affected by mutations in the hydrophobic substrate-binding pocket. In contrast to their effects on ligand binding, the effects of multiple mutations on product release are additititve (the points lie within the diagonal band), indicating that the individual mutations do not influence one another substantially in this step. The apparent lack of sensitivity of k_{off} (H$_4$F) and k_{rev} to comparatively subtle changes in side-chain interactions is consistent with product release and the reverse hydride-transfer step involving gross conformational changes in the enzyme's loop I substructure (Li et al., 1992), which may abolish the coupling between side chains at positions 28 and 54. The effects of multiple mutations on the hydride-transfer rate constants in the
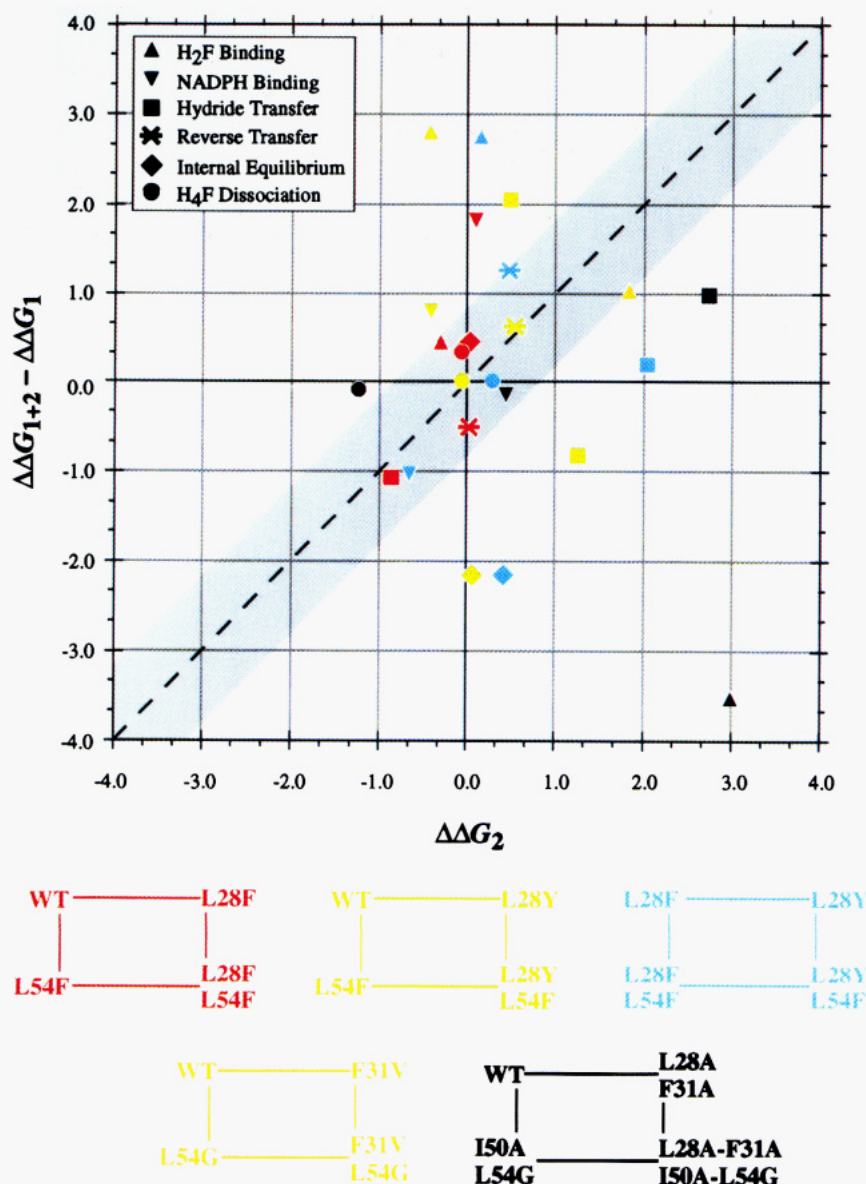
FIGURE 6: Plot of $\Delta\Delta G_{1+2} - \Delta\Delta G_1$ *versus* $\Delta\Delta G_2$ for the three mutational cycles investigated here in addition to the WT → F31V-L54G cycle (Chen et al., 1987; Mayer et al., 1986; Murphy & Benkovic, 1989; Taira et al., 1987; Wagner & Benkovic, 1990) and the WT → L28A-F31A-I50A-L54G cycle (Huang et al., 1994) reported previously. The values $\Delta\Delta G_1$, $\Delta\Delta G_2$, and $\Delta\Delta G_{1+2}$ are defined as the differences in free energy changes for the single mutant having the larger effect, the single mutant having the smaller effect, and the double mutant, respectively (Mildvan et al., 1992). The red, green, and blue symbols represent the same mutational cycles as in Figure 5, while the gold and black symbols represent the WT → F31V-L54G and WT → L28A-F31A-I50A-L54G mutational cycles, respectively. The diagonal line and the gray region are the same as those described in Figure 5. According to the definitions of Mildvan et al. (1992), the data points falling below the diagonal in the $(-x, -y)$ quadrant represent synergistic beneficial double mutational effects.

forward direction are more variable than for any other single step in the normal enzyme turnover cycle and reflect changes in the ground-state E·NH·H_2F complex as well as the transition state for the chemical step. The ability of the enzyme to bring the substrate and cofactor to the proper orientation for hydride transfer is sensitive to the interactions between distant side chains bridged by substrate.

As Figure 6 demonstrates, more than half of the mutational effects on rate or equilibrium constants for these sets of residue changes are nonadditive. However, for two-thirds of the parameters characterized, the net effects of multiple mutations are antagonistic or partially additive so that the observed parameters are closer to wild-type values than expected. The fact that there are no examples of synergistic enhancement of beneficial mutational effects [i.e., points

lying below the diagonal in the $(-x, -y)$ quadrant] is consistent with the expectation that the binding/active site surface has been optimized in the wild-type enzyme.

CONCLUSIONS

This work has focused on the additivity of mutational effects resulting from the L54F mutation in combination with either the L28F or the L28Y mutation. The simultaneous analysis of three interrelated mutational cycles (Figure 2) has allowed us to identify specific side-chain interactions involved in a particular catalytic step. Each of the single mutations results in an improved affinity for substrate (H_2F), presumably from an increase in favorable interactions when a leucine side chain is replaced by an aromatic side chain; however, these substitutions increase crowding and/or rigidity at the combining site so that pairs of mutations reduce the

enzyme's affinity for H_2F. The mutational effects on the forward and reverse hydride-transfer rates suggest that Phe28 and Leu54 cooperatively facilitate hydride transfer. Changing either of these residues eliminates the cooperativity and decreases the rate of hydride transfer. All mutations at positions 28 and 54 increase k_{off} (H_4F), and combined effects of pairs of mutations are essentially additive. Overall, the change in side chain from Phe28 to Tyr28 can alter interactions both with ligands and with the side chain at position 54. The latter effect suggests that a single functional group change, from $-H$ to $-OH$, can influence the additivity of mutational effects. The sensitivity of ΔG_I values for a given enzyme to a particular step suggests changes in the conformational state of enzyme which modulates the side-chain interactions.

Although the effect of most second mutations within the hydrophobic folate binding pocket of *E. coli* DHFR is to keep thermodynamic and kinetic parameters closer to the wild-type values than expected, the general rule is for the effects of two mutations to be nonadditive. Moreover, some pairs of mutations actually reverse the energetic perturbation of a particular step relative to the additive effect. To date, no examples of synergistically favorable double mutations have been reported. With an enhanced knowledge of the molecular origin of nonadditive effects, it may be possible to optimize an approach to improve the enzyme's efficiency by coupling mutations.

ACKNOWLEDGMENT

REFERENCES

Adams, J. A., Johnson, K., Matthews, R., & Benkovic, S. J. (1989) *Biochemistry 28*, 6611−6618.

Adams, J. A., Fierke, C. A., & Benkovic, S. J. (1991) *Biochemistry 30*, 11046−11054.

Appleman, J. R., Beard, W. A., Delcamp, T. J., Prendergast, N. J., Freisheim, J. H., & Blakley, R. L. (1990) *J. Biol. Chem. 265*, 2740−2748.

Baccanari, D. P., Averett, D., Briggs, C., & Burchall, J. (1977) *Biochemistry 16*, 3566−3572.

Barshop, B. A., Wrenn, R. F., & Frieden, C. (1983) *Anal. Biochem. 130*, 134−145.

Benkovic, S. J., Fierke, C. A., & Naylor, A. M. (1988) *Science 239*, 1105−1110.

Birdsall, B., Burgen, A. S. V., & Roberts, G. C. K. (1980) *Biochemistry 19*, 3723−3731.

Blakley, R. L. (1960) *Nature (London) 188*, 231−232.

Bolin, J. T., Filman, D. J., Matthews, D. A., Hamlin, R. C., & Kraut, J. (1982) *J. Biol. Chem. 257*, 13650−13662.

Bystroff, C., & Kraut, J. (1991) *Biochemistry 30*, 2227−2239.

Bystroff, C., Oatley, S. J., & Kraut, J. (1990) *Biochemistry 29*, 3263−3277.

Cayley, P. J., Dunn, S. M. J., & King, R. W. (1981) *Biochemistry 20*, 874−879.

Chen, J. T., Mayer, R. J., Fierke, C. A., & Benkovic, S. J. (1985) *J. Cell. Biochem. 29*, 73−82.

Chen, J. T., Kazunari, T., Tu, C. P. D., & Benkovic, S. J. (1987) *Biochemistry 26*, 4093−4100.

Curthoys, H. P., Scott, J. M., & Rabinowitz, J. C. (1972) *J. Biol. Chem. 247*, 1959−1964.

Dawson, R. M. C., Elliott, D. C., Elliott, W. H., & Jones, K. M. (1969) in *Data for Biochemical Research*, Oxford University Press, Oxford, England.

Dunn, S. M. J., & King, R. W. (1980) *Biochemistry 19*, 766−773.

Ellis, K. J., & Morrison, J. F. (1982) *Methods Enzymol. 87*, 405−426.

Fierke, C. A., & Benkovic, S. J. (1989) *Biochemistry 28*, 478−486.

Fierke, C. A., Johnson, K. A., & Benkovic, S. J. (1987a) *Biochemistry 26*, 4085−4092.

Fierke, C. A., Kuchta, R. D., Johnson, K. A., & Benkovic, S. J. (1987b) *Cold Spring Harbor Symp. Quant. Biol. 52*, pp 631−638.

Filman, D. J., Bolin, J. T., Matthews, D. A., & Kraut, J. (1982) *J. Biol. Chem. 257*, 13663−13672.

Hanahan, D. (1983) *J. Mol. Biol. 166*, 557−580.

Horovitz, A., & Fersht, A. R. (1990) *J. Mol. Biol. 214*, 613−617.

Howell, E. E., Warren, M. S., Booth, C. L. J., Villafranca, J. E., & Kraut, J. (1987) *Biochemistry 26*, 8591−8598.

Huang, Z., Wagner, C. R., & Benkovic, S. J. (1994) *Biochemistry 33*, 11576−11585.

Kallen, R. G., & Jencks, W. P. (1966) *J. Biol. Chem. 241*, 5845−5850.

Li, L., Falzone, C. J., Wright, P. E., & Benkovic, S. J. (1992) *Biochemistry 31*, 7826−7833.

LiCata, V. J., & Ackers, G. K. (1995) *Biochemistry 34*, 3133−3139.

Mathews, C. K., & Huennekens, F. M. (1960) *J. Biol. Chem. 235*, 3304−3308.

Mayer, R. J., Chen, J. T., Taira, K., Fierke, C. A., & Benkovic, S. J. (1986) *Proc. Natl. Acad. Sci. U.S.A. 83*, 7718−7720.

Mildvan, A. S., Weber, D. J., & Kuliopulos, A. (1992) *Arch. Biochem. Biophys. 294*, 327−340.

Murphy, D. J., & Benkovic, S. J. (1989) *Biochemistry 28*, 3025−3031.

Penner, M. H., & Frieden, C. (1985) *J. Biol. Chem. 260*, 5366−5369.

Penner, M. H., & Frieden, C. (1987) *J. Biol. Chem. 262*, 15908−15914.

Rabinowitz, J. C. (1960) in *The Enzymes* (Boyer, P. D., Lardy, H., & Myrback, K., Eds.) 2nd ed., pp 185−252, Academic Press, New York.

Seeger, D. R., Cosulick, D. B., Smith, J. M., & Hultquist, M. E. (1949) *J. Am. Chem. Soc. 71*, 1753−1758.

Stone, S. R., & Morrison, J. F. (1982) *Biochemistry 21*, 3757−3765.

Stone, S. R., & Morrison, J. F. (1983) *Biochim. Biophys. Acta 745*, 247−258.

Taira, K., & Benkovic, S. J. (1988) *J. Med. Chem. 31*, 129−137.

Taira, K., Fierke, C. A., Chen, J. T., Johnson, K. A., & Benkovic, S. J. (1987) *Trends Biochem. Sci. 12*, 275−278.

Viola, R. E., Cook, P. F., & Cleland, W. W. (1979) *Anal. Biochem. 96*, 334−340.

Wagner, C. R., & Benkovic, S. J. (1990) *Trends Biotechnol. 8*, 263−270.

Wagner, C. R., & Benkovic, S. J. (1992) *J. Med. Chem. 35*, 2912−2915.

Wagner, C. R., Thillet, J., & Benkovic, S. J. (1992) *Biochemistry 31*, 7834−7840.

Wells, J. A. (1990) *Biochemistry 29*, 8509−8517.